Index of Refraction Measurements for a Superluminal Radiation

by

James B. Carlton and William A. Tiller

Introduction

About 100 years ago, Maxwell derived a set of theoretical equations which governed the behavior of electromagnetic radiation. One of the predictions from these equations was the existence and harmonic behavior of radio waves emanating outwards from an antenna. When electrical charges on the antenna are accelerated, a train of electromagnetic waves travels outwards from the charges. An equally allowed solution to the Maxwell equations is a wave which travels inwards from large distances towards the antenna. However, this latter possible solution is generally rejected, because it does not correspond with our physical experience. It is considered to be rather strange to imagine that before charges are set in motion, a spherical wave starts out from infinity and arrives at the charges just at the time they begin to move.

Quite a different kind of wave, called magnetoelectric by one of us[4], is postulated to be generated by the motion of magnetic charges of etheric substance and travels at much higher speeds than electromagnetic waves. Thus, the magnetoelectric wave must be considered to be a superluminal wave relative to the reference frame of physical substance. This space frame for

physical substance has been called the positive space-time frame ((+) s/t), whereas the space frame for etheric substance has been called the negative space-time frame ((-) s/t)[4]. These two frames are thought to be conjugates to each other with a type of mirror image relationship existing between them. If we designate physical light (EM light) as operating within the (+) s/t frame, then its conjugate (ME light), having inverse properties, must operate within the (-) s/t frame. One of us (WAT) has further expanded on this, postulating that every quality of substance that exists in the physical world ((+) s/t frame) has a conjugate or mirror image quality embodied in the etheric world ((-) s/t frame); i.e., a Mirror Principle is operating between these two frames[4].

Table I provides a partial listing of qualities or properties associated with the (+) s/t frame and their conjugates in the (-) s/t frame. Such a listing theoretically predicts how the conjugate quality will appear or behave in the (-) s/t frame. Items 7-10 have been experimentally investigated with some degree of confirmation[1,2]. The experimental investigation of item 11 is the subject matter of the present paper.

One could say that, since the time of Maxwell, a foundation existed for describing (-) s/t physics. However, there are at least two basic reasons why this physics was not developed. One is that there were few reliable detectors of this "nonphysical" substance and radiation. The other is that the proper perspective for giving meaning to such observations was not available. These constraints do not seem to prevail today.

Several years ago, one of us (JBC) became involved in a line of research wherein the fundamental characteristics of a rather abstract type of energetics,

TABLE 1

COMPARISON OF SOME PROPERITES OF EVENTS IN THE (+) S/T FRAME VERSUS THE (-) S/T FRAME.

	(+) S/T FRAME EVENT	(-) S/T FRAME EVENT
1.	Basic atomic unit is built from electrical substance.	Basic atomic unit is built from magnetic substance.
2.	Entropy increases - (matter becomes disorganized).	Entropy decreases - (matter becomes organized).
3.	Major electrical and minor magnetic effects occur.	Major magnetic and minor electrical effects occur.
4.	Positive mass.	Negative mass.
5.	Time Flows in positive direction.	Time flows in negative direction.
6.	Concave lenses diverge light.	Concave lenses converge light.
7.	Convex lenses converge light.	Convex lenses diverge light.
8.	Velocities cannot exceed that of light.	Velocities are greater than that of light.
9.	Images seen in simple telescope are inverted.	Images seen in simple telescope are erect.
10.	Telescope magnifies.	Telescope demagnifies.
11.	Index of refraction for electromagnetic light >1.	Index of refraction for magnetoelectric light <1.

generally classified as auric phenomena, was being studied. This was a phenomena where children, serving as subjects, were capable of seeing auric light around animate and/or physical energy fields. That research, which is too voluminous to review here in its entirety[1-3], developed several techniques that were designed to elucidate some of the fundamental characteristics of the associated energy system involved. The bulk of that work centered around using a parallel-plate air-type capacitor and a controllable high-voltage D.C. power supply to develop an electric field across an air gap. Various and sundry colored auric manifestations appeared in these fields to the subject. These manifestations have been documented by experimentation to have some unusual properties[1-3]. Some of these properties are:

1. The physical energy field is an integral part of the pattern seen; thus, changes in the field intensity bring about changes in the observed pattern. Turning off the electric field causes the pattern to decay in a lawful manner.

2. The ambient physical light intensity was shown to have an influence upon the intensity of the pattern seen.

3. The frequency of the ambient physical light was shown to strongly influence the ability to see any pattern at all.

4. Scale measurements of particular shapes within the pattern viewed, both directly and via a telescope, resulted in a demagnified image with the telescope compared to direct observation--which is just opposite to our normal expectations with physical EM light.

The patterns seen within the physical energy field are theorized to be

formed by a type of diffraction phenomenon which involves the mind of the subject as well as ME radiation and may be detected by the (-) s/t sensory system of the children. A more detailed picture of the theoretical constructs that we apply to the present objective has been given by one of us[6], so only a very brief mention of two relevant aspects will be given here:

(1) From the mirror principle, as the physical mass density, m_p, increases, the etheric mass density, m_e, decreases so the EM light slows down as it enters lenses or prisms, whereas ME light speeds up.

(2) ME light and EM light do not directly interact with each other but do so via the deltron field[4] which serves as a kind of fluid clutch for energy transfer between these two types of radiation. The deltrons can travel at speeds both less than and greater than that of EM light.

Some general exploratory studies of this auric phenomenon that dealt with the spectral aspects of this energy system have been reported[1]. These studies incorporated the use of monochromatic light and sharp cut-off, gelatin-type filters. No specific conclusions could be drawn from the studies except that ample evidence was found that the visible EM spectrum was indeed involved. This conclusion warranted further systematic study of the spectral aspects of this energy system, which is carried out in the present work. The objective of this paper was to make a serious investigation of the index of refraction of the radiation associated with this type of auric phenomena.

Refraction Theory

When light falls upon the smooth surface of a transparent substance, like water or glass, part of it is reflected according to the law of reflection

and the rest is refracted (bent) into the medium. The bending is due to the reduction in velocity of the light upon entering the second medium. The direction of the refracted rays is measured by the angle they make with the surface normal.

The angle of refraction, r, has been experimentally determined to depend upon two factors: (1) The angle that the incident ray makes with the normal, i, and (2) the index of refraction, N, for the substance in question. The index of refraction, N, is by definition the ratio of the velocity of light in a vacuum (V_1) to the velocity of light in the medium (V_2); i.e., $N = V_1/V_2$. Since physical light has its maximum velocity in a vacuum (V_1) and since it is always slowed down in dense material to a velocity (V_2), it follows that $V_1 > V_2$ so that $V_1/V_2 = N > 1$. Conversely, if there existed a radiation that speeded up on entering the medium to a velocity (V_2^*), then $V_1 < V_2^*$ so that $V_1/V_2^* = N^* < 1$. According to Table 1, item 8, the (-) s/t conjugate of electromagnetic radiation; i.e., magnetoelectric radiation, is such a radiation. Thus, according to item 11, the index of refraction, N, for electromagnetic radiation is $N > 1$ and for magnetoelectric radiation, $N^* < 1$.

Snell has shown that, for any transparent substance, the ratio of the sine of the angle of the incident light (Sin i) to the sine of the angle of the refracted light (Sin r) is the same for all angles of incidence and is equal to the refraction index N[5]. This relationship is called Snell's law of refraction and is stated mathematically as

$$N = \frac{V_1}{V_2} = \frac{\text{Sin } i}{\text{Sin } r} \qquad (1)$$

Equation 1 does not directly lend itself to determining N for substances with nonparallel sides; i.e., for a prsim. However, it is possible to derive such a realtionship from this equation. Figure 1 schematically illustrates a prism and a collimated, monochromatic light beam I. The light beam I impinges upon the prism surface at point P and, if it were not for refraction, would traverse the line POK. However, refraction by the prism causes the physical beam to take the path PS through the prism and emerge from the latter at point S. At S, the velocity of the beam increases and travels the path SQ. Point A of the prism is called the refracting angle and point O is designated as the prism center of rotation. If the light beam and prism are situated approximately as shown, slight rotations of the prism about point O in either a clockwise or counter-clockwise direction produces a variation in the refraction angle, $+D_m$, the resulting angle ($+D_m$) is called the angle of minimum deviation. If these conditions are met, it can be shown that the derivation of the index of refraction, by use of Snell's law, is given by the equation[5]

$$N = \frac{\text{Sin } \frac{1}{2} (A + D_m)}{\text{Sin } \frac{1}{2} A} \qquad (2)$$

In practice, the angles A and $+D_m$ are determined experimentally and N is computed from eq. 2.

According to the (-) s/t theory, there must exist a conjugate beam that is the mirror image of beam I'. The mirror image beam I^* is thus generated if the plane of the page of Fig. 1 is folded along the line POK so that the line SQ fixes the location of a new line TR; i.e., I^* is the mirror image of

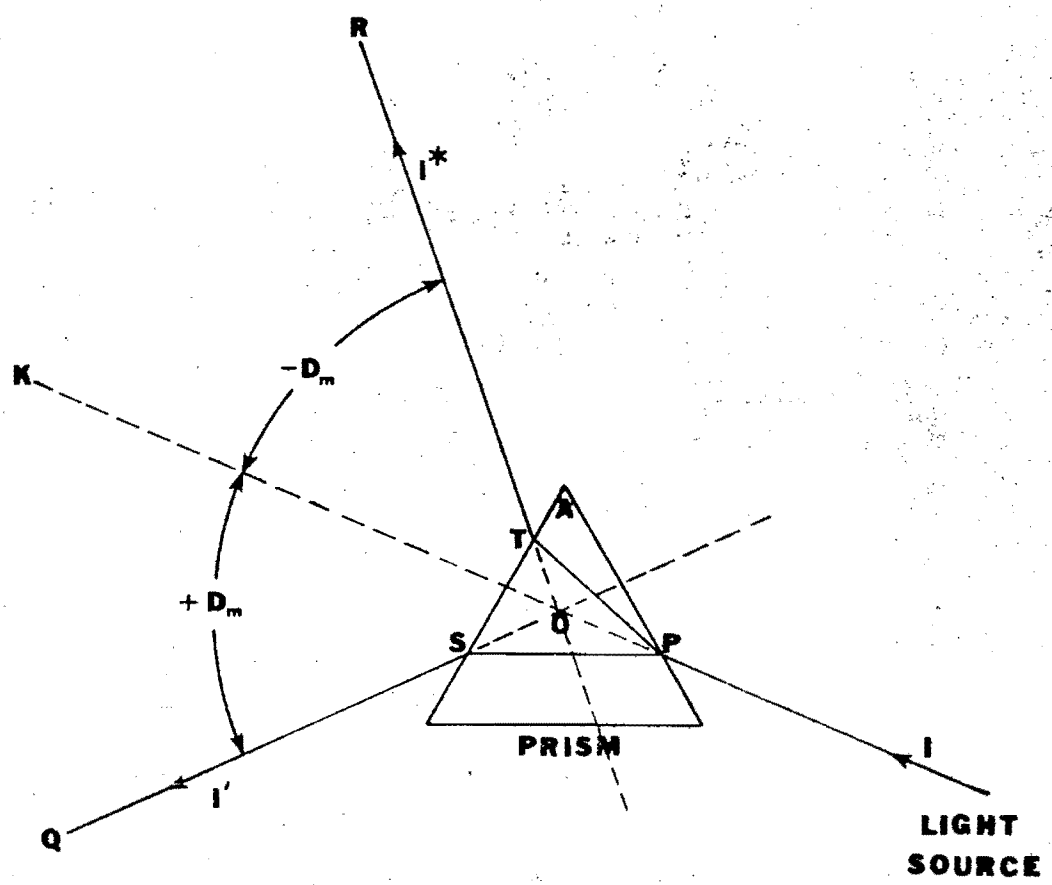

Fig. 1. Schematic diagram illustrating the prism refraction of a collimated, monochromatic light beam and its associated mirror image.

I'. Since the straight line projection of line TR must go through the prism center 0 forming the line 0TR, the path that the conjugate beam takes through the prism is obtained by joining points T and P. Thus the physical light beam I' takes the path PSQ through and out of the prism while that for the conjugate beam I^* is PTR.

For a given prism, the angle A is fixed. Thus, from eq. 2, N is noted to vary according to the angle $+D_m$. For example, if there was not diffraction of the beam by the passage through the prism, then $+D_m = 0$ and

$$N = \frac{\text{Sin } \frac{1}{2} (A + 0)}{\text{Sin } \frac{1}{2} A} = 1 \qquad (3)$$

If we let the line I' represent the graph of a simple linear function, $y = f(x)$, with the line POK the positive x-axis, and a line perpendicular to it and passing through 0 the appropriate positive y-axis, then $y = f(x)$ has a positive slope and thus $+D_m$ designates a positive angle. Therefore, the mirror image of $y = f(x)$ will have a negative slope; i.e., $y^* = f(x)$, and hence a negative angle of minimum deviation, $-D_m$. This reasoning leads directly to the alteration of eq. 2 to give

$$N^* = \frac{\text{Sin } \frac{1}{2} (A - D_m)}{\text{Sin } \frac{1}{2} A} \qquad (4)$$

From eq. 4, it is now possible to compute N^* for any angle, $-D_m$, as shown in Fig. 1.

Method of Investigating N^*

Additional theoretical aspects that appropriately come under methods need

to be considered. These considerations deal with the question--What insights does the (-) s/t theory provide as to the expected experimental value(s) for N^*? This question was considered both from a theoretical standpoint and on the basis of previous experimental results.

The decision was made to use two prisms with distinct N-values to investigate N^*. Access to a spectroscope permitted the experimental measurement of N for the two prisms. The light source used in this phase was a sodium lamp. The bright yellow line in the sodium lamp spectra was the one used in the present case. The experimental results obtained by measuring the refraction angle, A, the angle of minimum deviation, $-D_m$, and the computed value for N for each prism were

1. $A_1 = 60^o$, $D_{m,1} = 50.93$, $N_1 = 1.648$

2. $A_2 = 45^o$, $D_{m,2} = 29.25$, $N_2 = 1.577$.

Next, the values for $D_{m,1}$ and $D_{m,2}$ were substituted into eq. 4 to compute the associated N_1^* and N_2^* values. These were found to be

1. $N_1^* = 0.16$

2. $N_2^* = 0.36$.

The latter values of N^* are, therefore, those to be expected from theory if the physical light source is that previously described.

However, if the children are not observing the ME beam directly but are instead observing the deltron beam which has been accelerated by the ME beam, then the observed values for the index of refraction should fall between the values of N and N^* given above.

The next part of the question dealing with expected N^* value(s) came about from considering previous research data dealing with "The Telescope Phenomena"[2]. Though the (-) s/t theory predicts a demagnification effect (see item 10, Table 1), unfortunately, it does not tell us much about the limits of this effect. In that research, a telescope was used that had a magnification power of 7. Thus, the main question here is whether the (-) s/t conjugate (demagnification effect) for a telescope with a physical magnification of 7 is one with an expected demagnification of 7 or not. In any event, the experimental data from the telescope work showed the phenomena to have a range (see Tables 2 and 3 of ref. 2) from a slight magnification of 1.5 to a demagnification of about 14 times. While it was true that most of the observations were below a demagnification value of 7, there was no firm indication that it was an expected limiting value either. Regardless of these probing questions, the important point is that there was a range over which the phenomena varied--which is currently believed to be involving the deltrons and to be reflecting the state of consciousness of the individuals at the time of experimentation. That is, we know that there are many different states of human consciousness. Since the mind is constructing the observed holographic auric images, there must be varying quantities of (-) s/t energy input. Apparently, the construction process cannot begin to take place until its human originator begins to move away from a consciousness state in which the (+) s/t sensory is fully functioning; i.e., (-) s/t is less a reality, to one in which his (-) s/t sensory system is beginning to operate; i.e., (+) s/t is less a reality. Between the extremes of the two conjugate sensory systems

TABLE 2

EXPERIMENTAL DATA FOR INDEX OF REFRACTION MEASUREMENTS

Rep.#	Date	$(D_{min.})^{\circ}$	$(D_{max.})^{\circ}$	$N^{*}_{min.}$	$N^{*}_{max.}$	$(Prism)^{\circ}$
			Subject: Len			
1.	8/3/75	(-) 5.25	(-)18.00	0.89	0.61	A = 45
		(+)17.00	(-)12.40	1.25	0.81	A = 60
2.	8/30/75	(-) 2.50	(-)23.00	0.95	0.50	A = 45
		(+)30.00	(-)19.00	1.41	0.70	A = 60
3.	9/10/75	(+) 6.25	(-)12.00	1.14	0.75	A = 45
		(+)11.00	(-)13.50	1.16	0.79	A = 60
4.	9/14/75	(+) 7.00	(-)32.75	1.15	0.28	A = 45
		(+)12.00	(-)12.00	1.18	0.81	A = 60
5.	9/27/75	(+) 8.25	(-)23.25	1.18	0.50	A = 45
		(+)23.25	(-)20.25	1.33	0.68	A = 60
6.	10/21/75	(+)13.75	(-)25.50	1.29	0.45	A = 45
		(+)24.75	(-)14.20	1.35	0.78	A = 60
7.	11/15/75	(+)20.50	(-)16.00	1.42	0.66	A = 45
		(+)18.25	(-)18.50	1.26	0.71	A = 60
8.	11/29/75 8:00 P.M.	(+)18.50	(-) 9.00	1.27	0.86	A = 60
9.	11/29/75 10:45P.M.	(+)30.00	(-)10.00	1.41	0.85	A = 60
10.	12/7/75	(+)30.50	(-)22.25	1.42	0.65	A = 60
			Subject: David			
1.	9/10/75	(+) 8.50	(-)17.25	1.18	0.63	A = 45
		(+) 5.50	(-)15.75	0.85	0.75	A = 60
2.	9/14/75	(+) 0.25	(-)22.50	1.00	0.51	A = 45
		(+)12.25	(-)19.00	1.18	0.70	A = 60
3.	10/21/75	(+)16.25	(-) 5.50	1.34	0.89	A = 45
		(+)14.75	(-) 8.50	1.21	0.87	A = 60
4.	11/29/75 8:00 P.M.	(+) 1.25	(-)17.50	1.02	0.72	A = 60
5.	11/29/75 10:45P.M.	(+)13.50	(-) 9.50	1.20	0.85	A = 60

Table 2 Contd.

			Subject: Bobby			
1.	11/15/75	(+)14.25	(-)22.75	1.21	0.64	A = 60
		(+) 1.25	(-)16.00	1.03	0.66	A = 45
2.	11/15/75	(+)18.00	(-)23.00	1.26	0.63	A = 60
3.	11/29/75	(+)14.00	(-)25.25	1.20	0.60	A = 60
4.	11/29/75	(+)16.25	(-)30.50	1.23	0.51	A = 60
5.	12/13/75	(+)17.50	(-)28.00	1.25	0.55	A = 60
			Subject: Douglas			
1.	8/3/75	(-) 5.25	(-)21.00	0.89	0.55	A = 45
		(+)24.50	(-) 5.75	1.34	0.91	A = 60
			Subject: Jennifer			
1.	12/6/75	(+)27.00	(-)16.50	1.38	0.74	A = 60
2.	12/6/75	(+)42.00	(-)32.00	1.55	0.48	A = 60
			Subject: Jan			
1.	12/6/75	(+)24.50	(-) 8.00	1.34	0.88	A = 60
2.	12/6/75	(+)28.00	(-)22.00	1.39	0.65	A = 60

lies a broad spectrum of different consciousness states and it is the understanding of the transition from one extreme to the other where our present knowledge is considerably lacking. Thus, from theory one can only anticipate a given N^* value for a fixed electromagnetic light frequency and a given prism; i.e., with the sodium light and the two prisms for which $N_1 = 1.648$ and $N_2 = 1.577$, $N_1^* = 0.16$ and $N_2^* = 0.36$. However, if the experimental results of the telescope phenomena are of any value in predicting N^* value(s), we might reasonably expect a range of values; i.e.,

$$N_1 = 1.648 > N_1^* \geq 0.16 \qquad \text{or} \qquad N_2 = 1.577 > N_2^* \geq 0.36 \ .$$

Thus N^* can be ≥ 1 or ≤ 1. In these inequalities, there is an experimental basis for $N \neq N^*$. This basis will be presented in the last section of this paper. After the experimental data is presented, we shall return to these considerations to see the extent to which the predictions were upheld.

There was a considerable amount of exploratory research activity involved in developing the method of investigating N^*. While much of the activity would be of a historical nature and not of particular importance, some of it is important in fully understanding the method developed and used. Basically, the idea was to approach the problem by use of a spectroscope. The essential parts of a spectroscope are a collimated beam of light originating from a suitable source passing through a narrow slit, a prism whose index of refraction is to be determined, and an appropriate scale for observing and measuring the refracted light deviation angles, $+D_m$. For a spectroscope that uses the human eye as the detector, the observations are made by the use of a telescope focused upon the narrow light entrance slit.

Fig 2

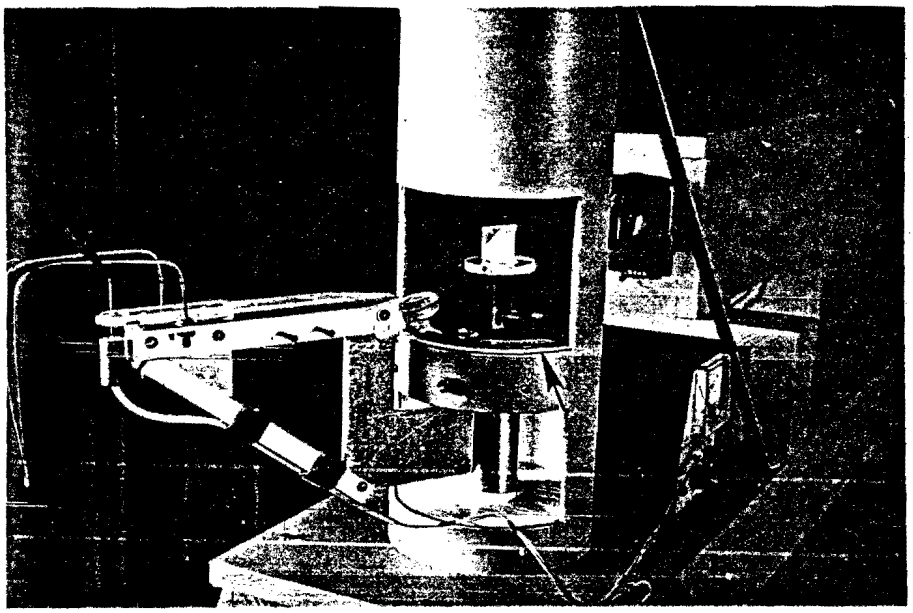

Fig. 2. Photograph illustrating some of the mechanical details of spectroscope constructed to study N^*.

The telescope is free to rotate about a point that coincides with the prism center of rotation and also in the plane of the incident and refracted light beam. A circular scale, graduated in degrees, is affixed to the telescope carriage or rotation assembly to provide for determing $+D_m$.

A spectroscope possessing these same important features was constructed for the current work with several modifications. An incandescent, collimated light source was used as the illuminating beam. The narrow light entrance slit, and the telescope used to observe it, were found to be unnecessary and impractical and were not used. In place of the telescope, a small ($\approx$ 0.5 mm diameter) fiber optic tube was attached to a rotatable arm to serve as a reference or alignment device for the subject to use. The fiber optic tube was rigidly fastened to the rotating arm by inserting it through a small stainless steel capillary tube (see arrow tip at left in Fig. 2). Also seen in this figure is the collimated light source (on the right), the prism affixed to a rotating pedestal (center of photograph), and the rotating arm supporting the fiber optic alignment point (on the left). The horizontal angular measurements were made possible by attaching a graduated protractor at the base of the prism pedestal (see second arrow, near center of Fig. 2). An index point mounted on the rotating arm, below a small magnifier and slightly above the graduated protractor, provided for sufficiently accurate angular readings. The loop of bent wire attached to the exterior end of the rotating arm permitted a subject to rotate the latter by simply holding to the wire and moving it to the right or left.

There was one major addition to the spectroscope--the prism was inserted

into a dc electric field. Figure 3 shows the general schematic layout that incorporated this feature. The electric field was experimentally found to be necessary to facilitate seeing the auric effect. This will be described in detail later. In order to incorporate the electric field feature within the spectroscope, the vertical cylinder seen in Fig. 2 was added. Two circular aluminum discs (14 cm diameter) were mounted horizontally (12 cm apart) in the cylinder. The prism was positioned in the approximate geometric center between the plates. Positioned thus, the plates had a 12 cm vertical separation distance. A 12.5 kV dc power supply was mounted in the upper part of the vertical cylinder which supplied the potential for the electric field. Two additional views of the complete spectroscope are shown in Figs. 4 and 5. A mobile stool was provided for a subject to sit upon as he or she looked into the prism.

Reference to Fig. 1 is again needed to describe more completely the experimental procedure. In the early exploratory phases, it was not at all clear to the investigator just what the children subjects were to look for and where. There were, however, two bits of information to go on: (1) From the mechanics of the spectroscope, the energy must pass through the prism for refraction to take place, and (2) previous research experience investigating auric phenomena suggested that perhaps the youngsters might look for a similar effect occurring within the prism. In the latter case, it is helpful to remember that the auric images are constructed by the mind of the test subject. From these suggestions and experimentation, a workable procedure was finally arrived at. The subject sits as some point k (see Fig. 1) and is

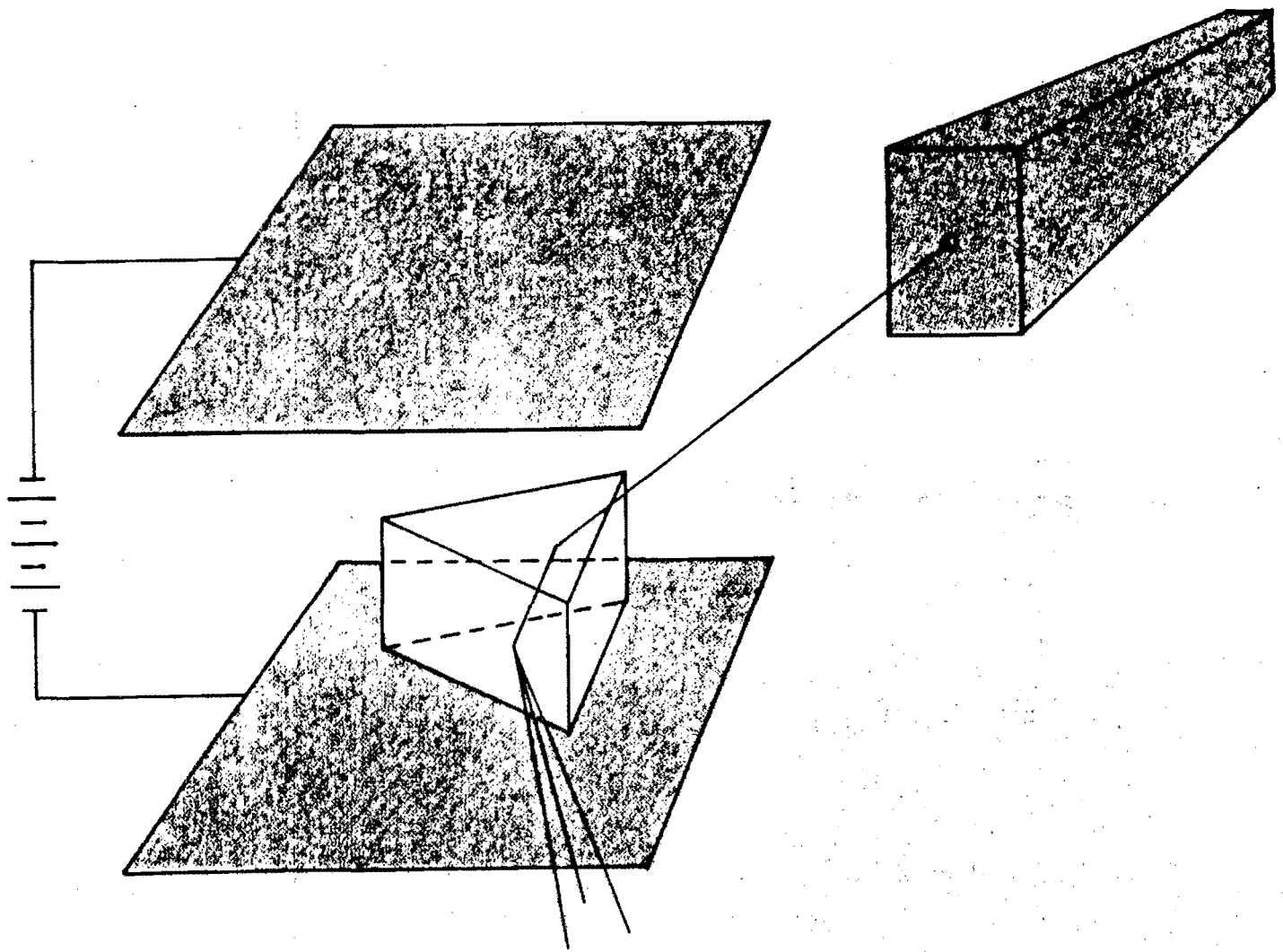

Fig. 3. Pictorial view showing orientation of prism, collimated incandescent light beam and the superimposed dc electric field.

Fig. 4

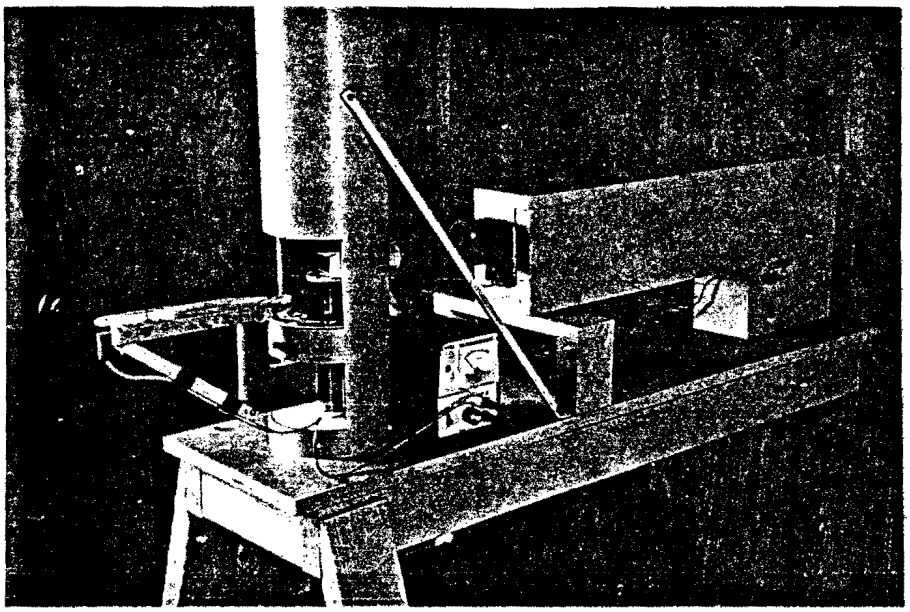

Fig. 4. Photograph of detailed relationship of collimated light source (right) and spectroscope (left).

Fig. 5

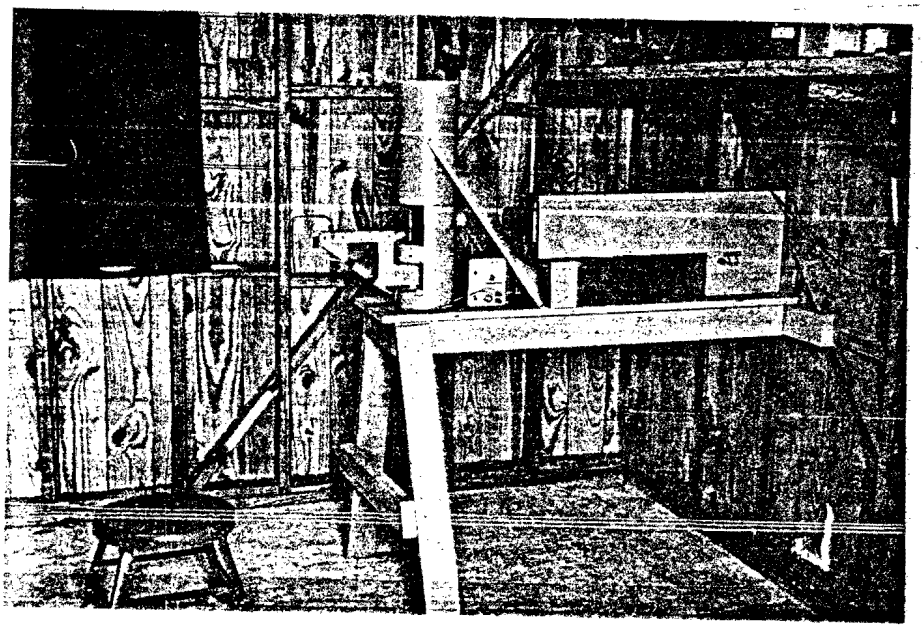

Fig. 5. Photograph of general view of complete spectroscope.

instructed to focus his/her attention on point P. (Note: The light beam I impinges on the prism at point P and has a diameter of about 1 mm. Points P and S, as well as the faint shaft of light connecting the two, are physically quite obvious (if all the other lights are off) when observed through the prism from an approximate position of point k.) Then the subject is instructed to look for an auric effect around point P.† It was subsequently found that, if the subject shifts on the stool toward some point R, then the auric image could only be observed to exist (be be "seen") through some fixed angle. For example, a typical result might be the case where an individual could only see the auric image around point P through the continuous angle of from $-D_m = 10^o$ to $-D_m = 20^o$. The shaded part of Fig. 7 illustrates this inclusive angle. To determine this angle, the subject first establishes visually where the image can and cannot be seen as he shifts laterally on the stool through some large arc. In the case above, for example, any position along the arc to the left of -10° or any position along the arc to the right of -20°, the auric image cannot be seen. After establishing these boundary positions, the subject then rotates the arm containing the fiber optic reference marker to a position that is in line with their eye and the point P. The angle indicated on the protractor is then read. This is followed by repeating the procedure for the other extreme boundary position.

---

†Some samples of the variety of colored sybmology that the subjects have seen are given in Fig. 6. The appended notes on color(s) of the manifestation and figure caption give clarifying details.

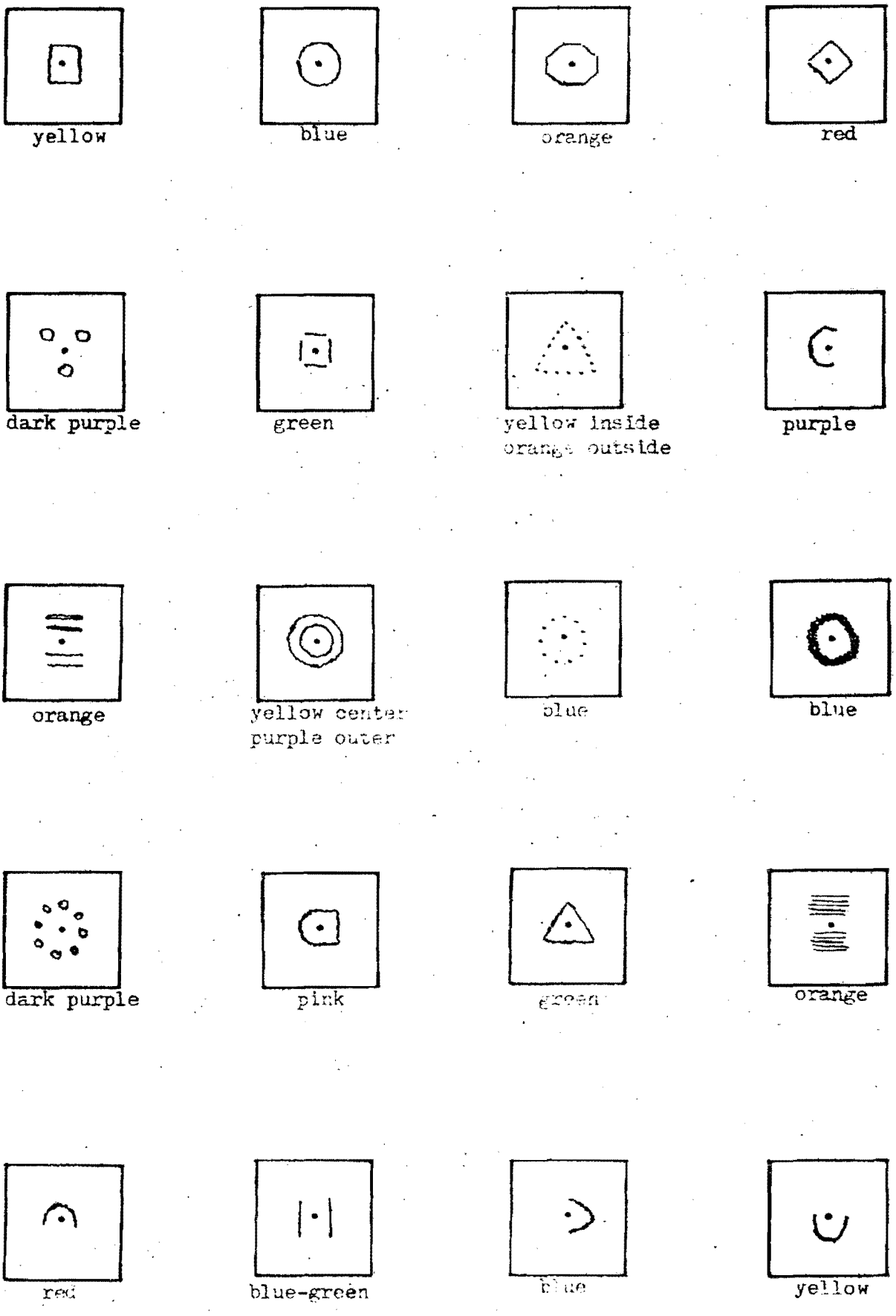

Fig. 6. Sketches of variety of symbology seen by subjects at rear of air-prism interface (outer square) and around physical light impingement point P (center dot).

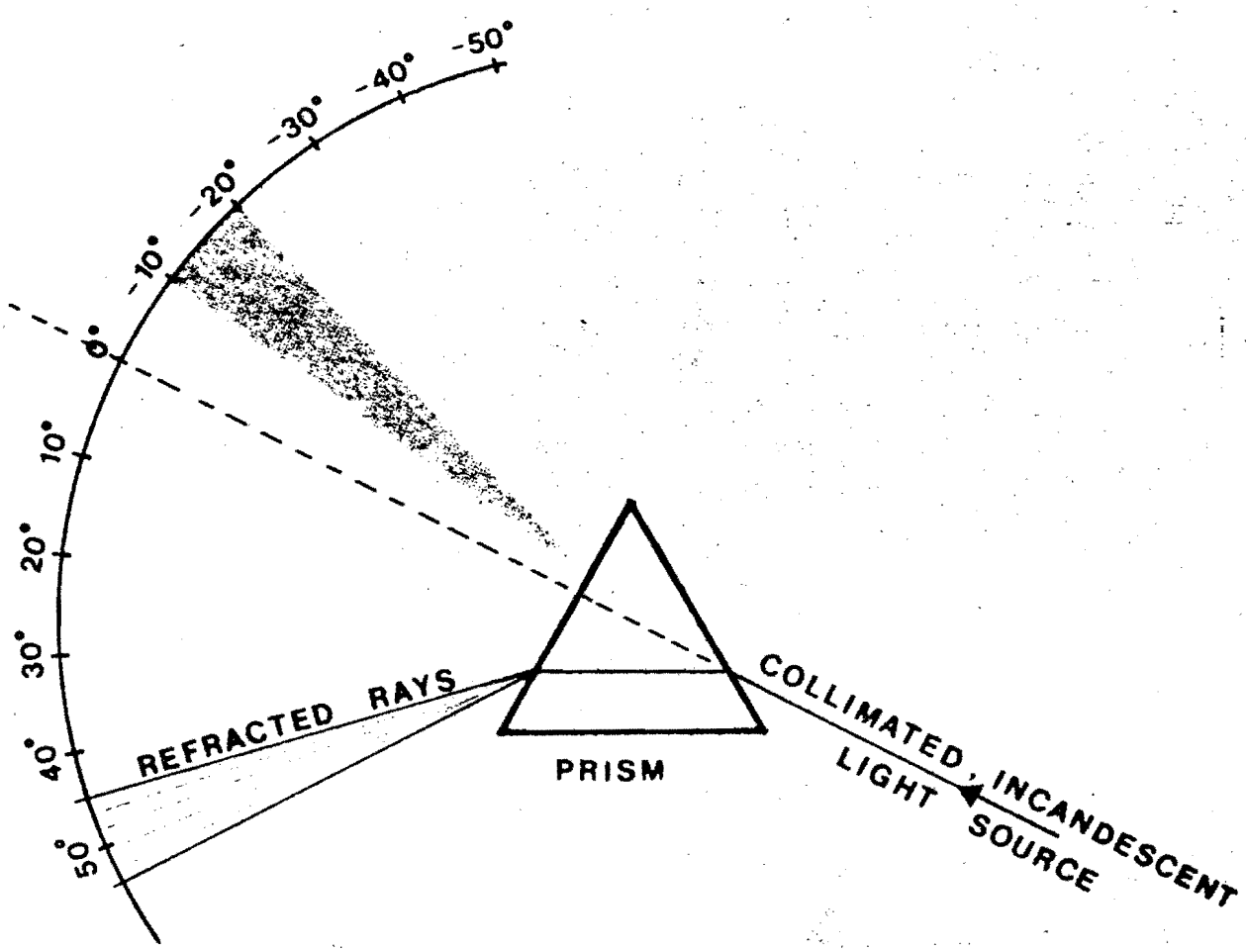

Fig. 7. Schematic diagram showing prism angular dispersion of (-) s/t radiation (shaded region) as typically perceived by a subject.

The superimposed electric field upon the prism now needs some elaboration. In the early experimental phases to work out the method of measuring N^*, the electric field was not used. In fact, it was not thought to be necessary. Though several children were used who had varying levels of sensitivity to this phenomena, none of them appeared to be able to see anything of value. From previous experience with these same youngsters, an intense physical energy field had almost always been used in the experiment. It had long ago been established that the field played the part of an amplifier--making it easier for the individual to see the various auric images. This experience suggested that an electric field superimposed upon the general region of the prism might facilitate what was sought. This turned out to be the case and the use of the electric field, as described, accounts for its incorporation.

The children (10-15 years old) used in the present work have all been used in previous work in varying amounts. Since the technique has been worked out, we find that others can readily do the same kind of thing. All of the experimentation to date has been designed to obtain data that would reveal the variation that will be encountered from the use of a few subjects with considerable replication. Also, the experimental method had incorporated several additional subjects so that variation, not only from a given subject, but among subjects, could be ascertained. That procedure is still being followed.

N^* Values with Prisms

The method delineated in the previous section was subsequently followed

throughout the experimental period. A total of six subjects were used. Table 2 shows the data collected for each subject. For the first subject, Len, there was a total of 10 replications (Rep. # in first column) using the 60° prism, N = 1.648, and 7 reps using the 45° prism, N = 1.577. The date of the experiment is given in the second column. The third column, $(D_{min.})^{o}$, was the angle of minimum deviation measured from the line of projection (POK) of the incident ray I of Fig. 1. For example, the first value of $(D_{min.})^{o}$ for Len of Table 2 gives a value of (-) 5.25^{o}. This means that the shaded arc of Fig. 7 would have its left (minimum) boundary line at (-) 5.25^{o} rather than (-) 10°, as shown. Also, the fourth column of Table 2, $(D_{max.})^{o}$, has its first value of (-) 18° and, accordingly, has its right (maximum) boundary line at this angle rather than (-) 20°, as shown in Fig. 7.

The inclusive angle from (-) 5.25^{o} to (-) 18.0^{o} means that Len could see the auric effect at point P continuously throughout this arc. To the right or left of these boundary lines, he could not see the effect even though the physical light impingement point P was visible beyond these boundaries.

Column 5 of Table 2, $(N^{*}_{min.})$, gives the values of N^{*} computed from eq. 4 for the angle $(D_{min.})^{o}$. For example, the first value of $N^{*}_{min.}$ in Table 2 is 0.89. This comes from eq. 4 when substituting the $-D_{m}$ value of 5.25^{o} and appropriately solving using the prism "A" value (see Fig. 1 locating angle A) shown in the last column of Table 2. Also, the $N^{*}_{max.}$ value (column 6) is solved similarly by substituting the $(D_{max.})^{o}$ value; i.e., for the example

above, $N^*_{max.} = 0.61$. The data on the second line of Table 2 was obtained immediately after the first line with the prism for which $A = 60^o$. From the $(D_{min.})^o$ column, it is obvious that some of the angles had positive values; i.e., $(+D_{min.})^o$. This means that that particular boundary line lies to the left of the line POK of Fig. 1. In those cases, eq. 2 is used to compute $N^*_{min.}$.

Prism Studies of the Superluminal Energy Spectrum

It is well known that if a collimated beam of white light is focused upon a prism, the refraction process separates the different color components of the light into a spectrum. The prism separates the light in accordance with the velocity of the components making up the light. The higher the velocity, the smaller is the refraction angle. Similarly, the lower the velocity, the greater the angle of refraction. Thus, in the ordinary visible spectrum, violet light has the lowest velocity and hence greatest refraction angle, while red light has the greatest velocity and smallest refraction angle. The remainder of the spectral colors, accordingly, have intermediate velocities and refraction angles. This information is schematically illustrated in the lower half of Fig. 8.

If, as previously described in Fig. 1, the page of Fig. 8 is folded along the line OP, the physical spectrum maps onto the upper part of the page, as shown. The mapping so produced is called the conjuage or mirror image of the physical spectrum. From the figure, Red maps onto Red*, Orange onto Orange*, etc. This implies that (-) s/t energy refracting in a prism

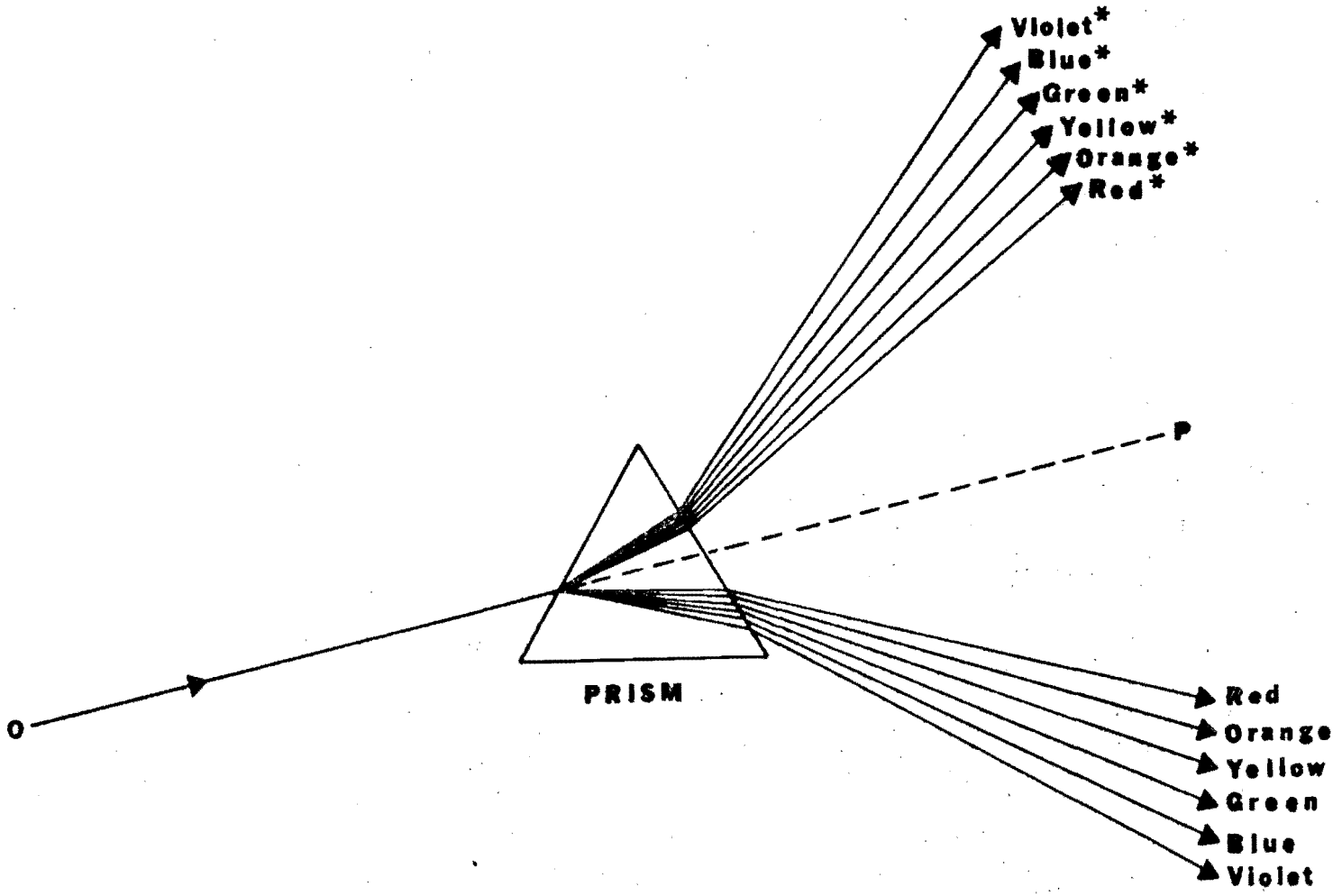

Fig. 8. Prism spectral dispersion of incandescent light (lower part of figure) and its mirrow image (upper portion).

will show spectral effects. Efforts were next made to study this theoretical expectation.

As before, the procedure was basically the same as for the N^* studies. The individuals observed that the auric effect at point P (Fig. 1) changed colors abruptly as they swept through the continuous arc in which the effect was visible. A series of tests were run where, in addition to measuring the extreme angular boundaries of the continuous arc, the angular boundaries of each color seen within the major arc were measured. Five schematic drawings representing typical results obtained from different individuals are shown in Figs. 9-13. For each color boundary line, the N^* values were computed and are shown on the figures. The colors, as perceived by the subjects for the regions between adjacent boundary lines, are given in the figure captions. The color sequence reads clockwise from the prism center.

Discussion of Results and Conclusions

How does the experimental data for N^* compare with the range predicted by theory and the experimental results of earlier work? The ranges for the expected values of N^* for the two prisms were

1. $A = 60^\circ$: $N_1 = 1.648 > N_1^* \geq 0.16$ and

2. $A = 45^\circ$: $N_2 = 1.577 > N_2^* \geq 0.36$.

From a review of the data in Table 2, for which $A = 60^\circ$, the following inequality is obtained:

$$1.55 \geq N_1^* \geq 0.48 \quad .$$

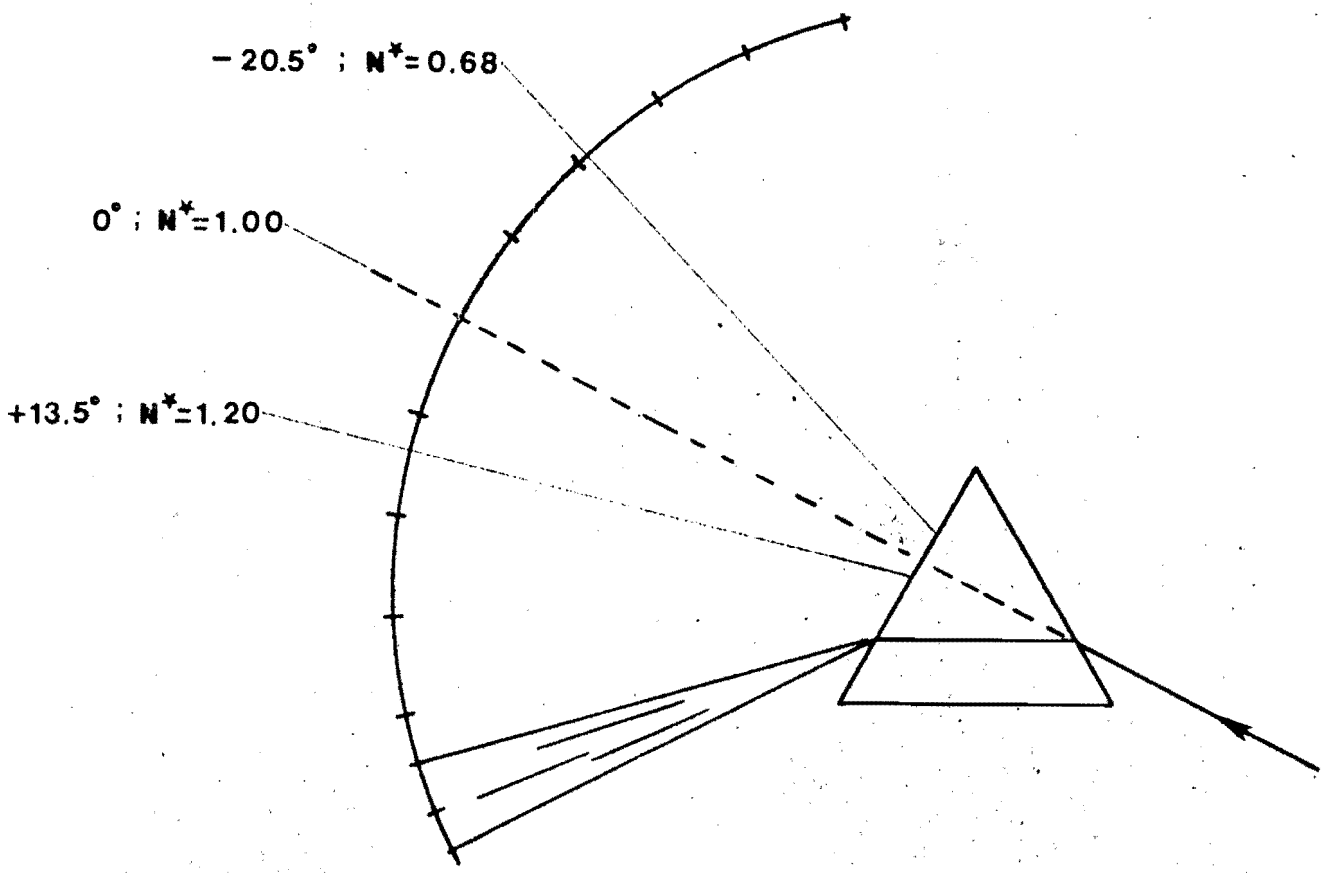

Fig. 9. Prism spectral dispersion of (-) s/t radiation as perceived by subject David F. (Colors reading clockwise about center of prism are yellow in the region from +13.5° to 0° then green in the region from 0° to -20.5°).

Fig. 9
Len

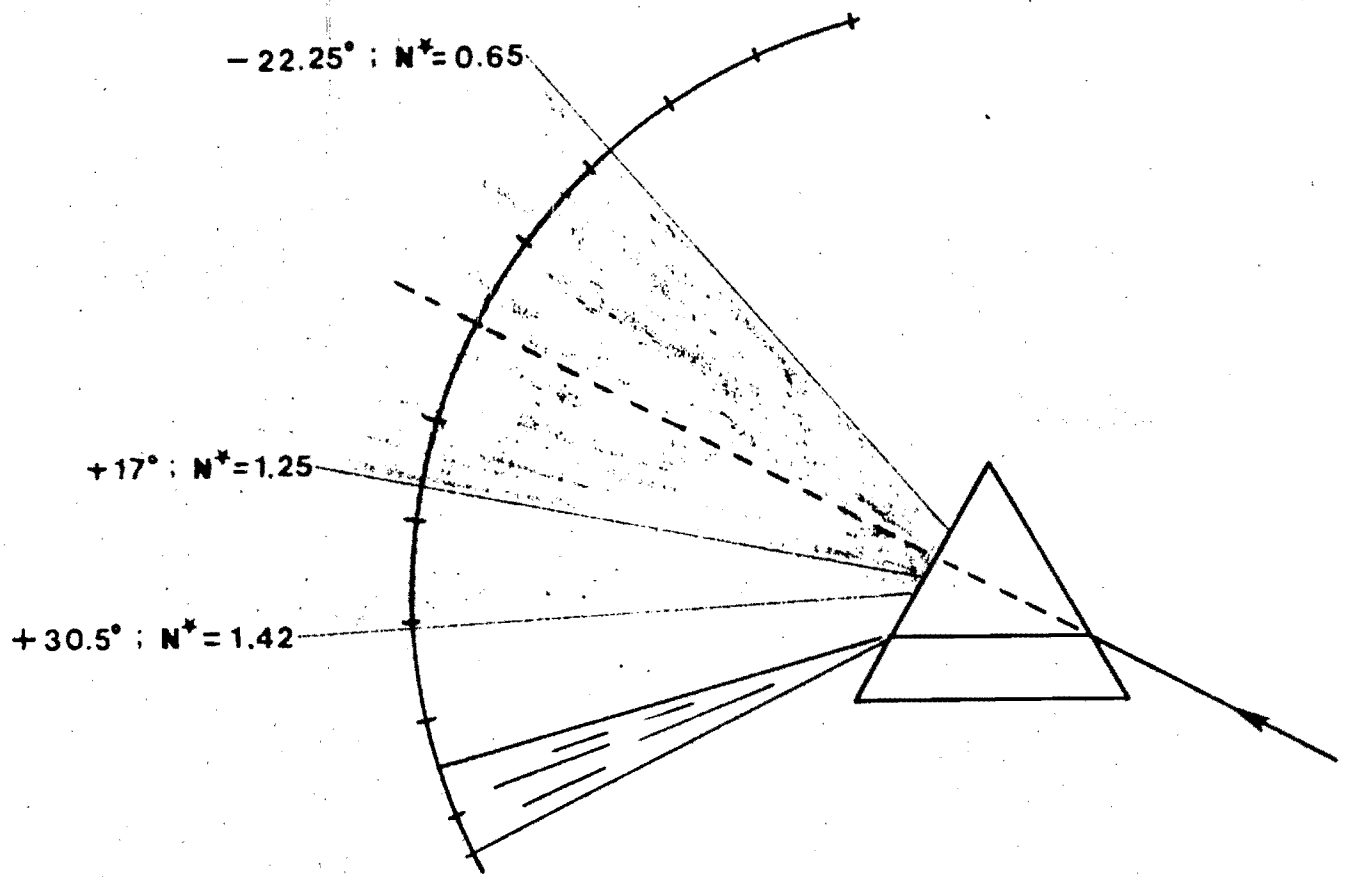

Fig. 10. Prism spectral dispersion of (-) s/t radiation as perceived by subject Len C. (Colors reading clockwise about prism center are blue - then purple).

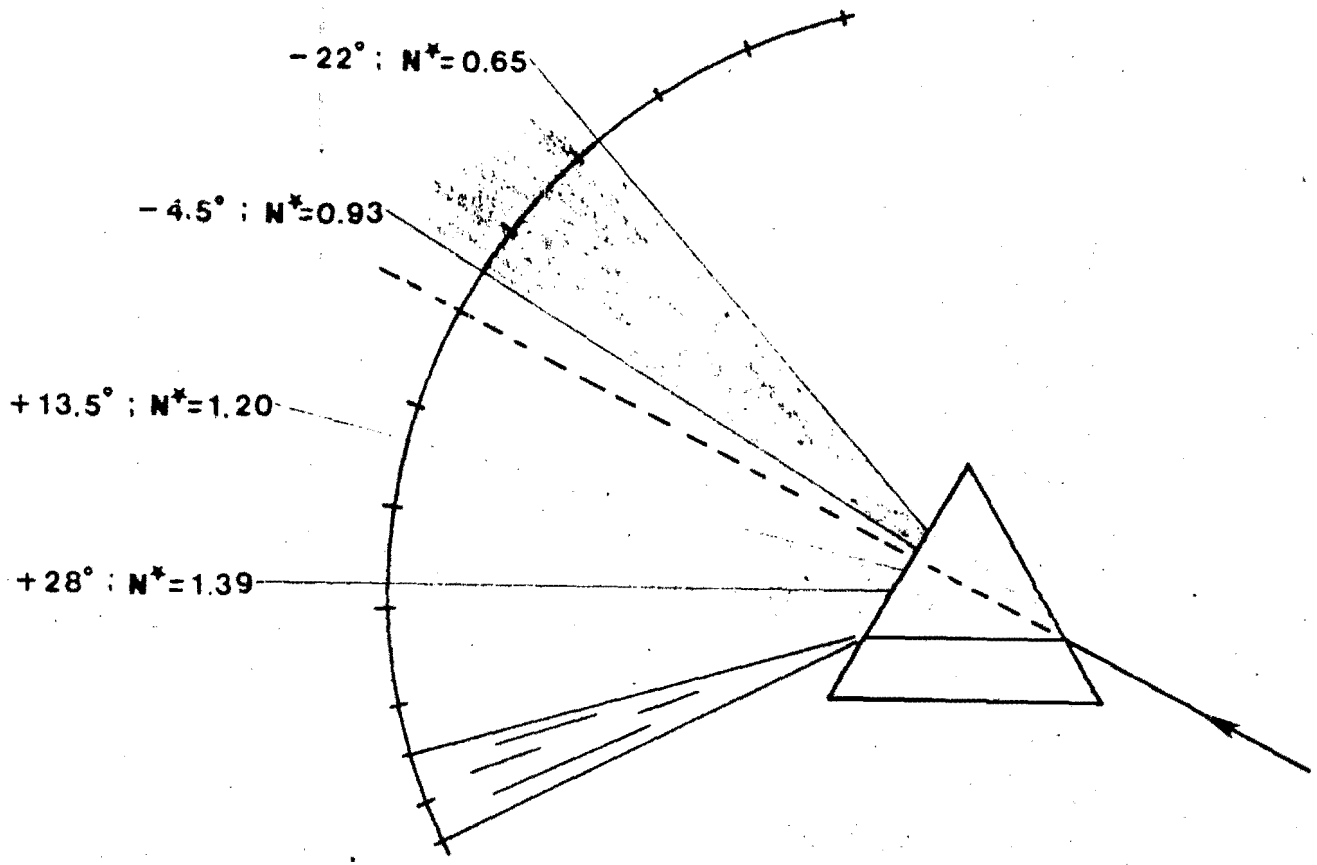

Fig. 11. Spectral dispersion of (-) s/t radiation as perceived by Jan J. (Colors reading clockwise are green - yellow - purple).

Fig. #
Jenny

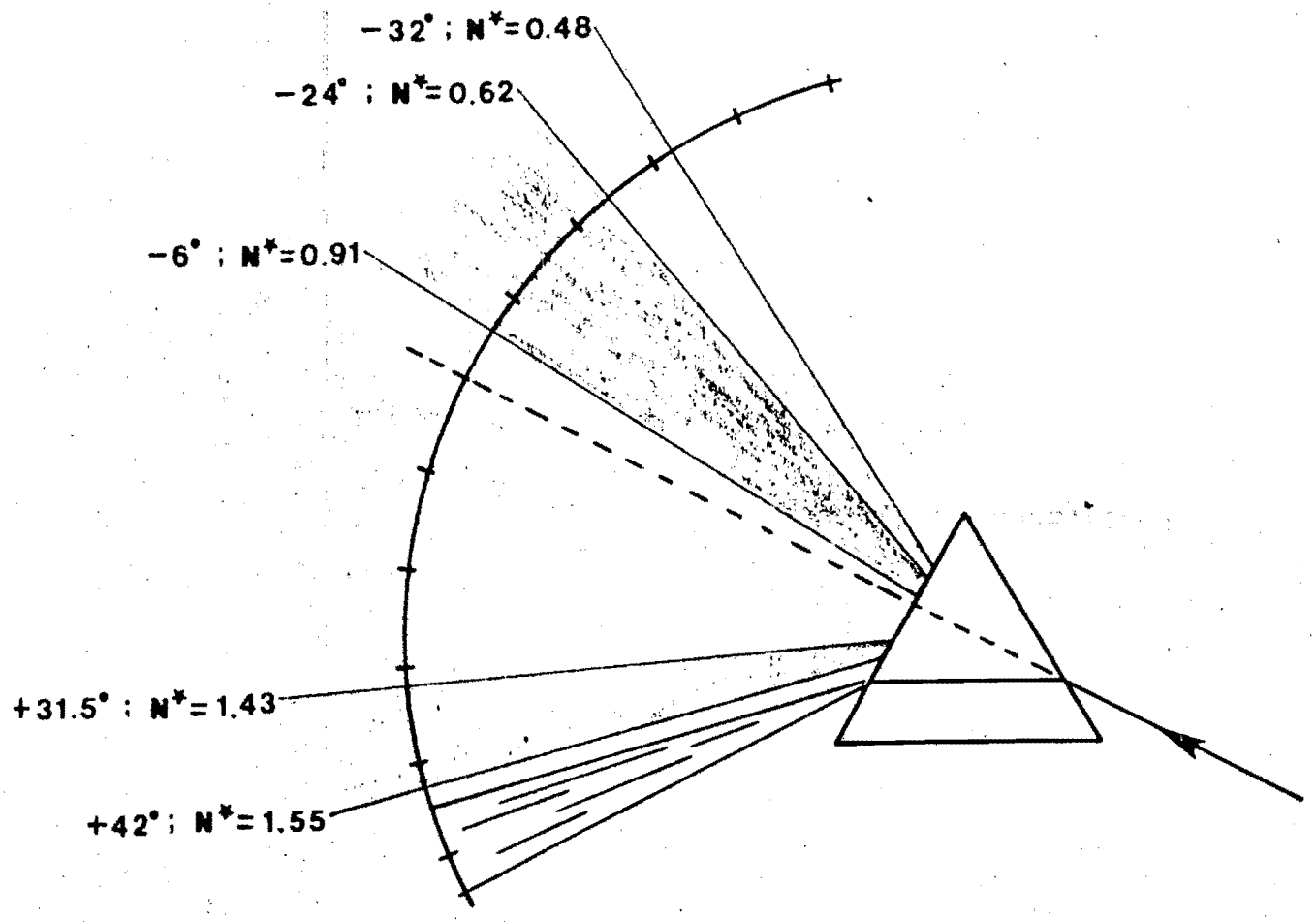

Fig. 12. Spectral dispersion of (-) s/t radiation as perceived by Jennifer P. (Colors reading clockwise are red - yellow - purple - blue).

Fig 13
Bobby

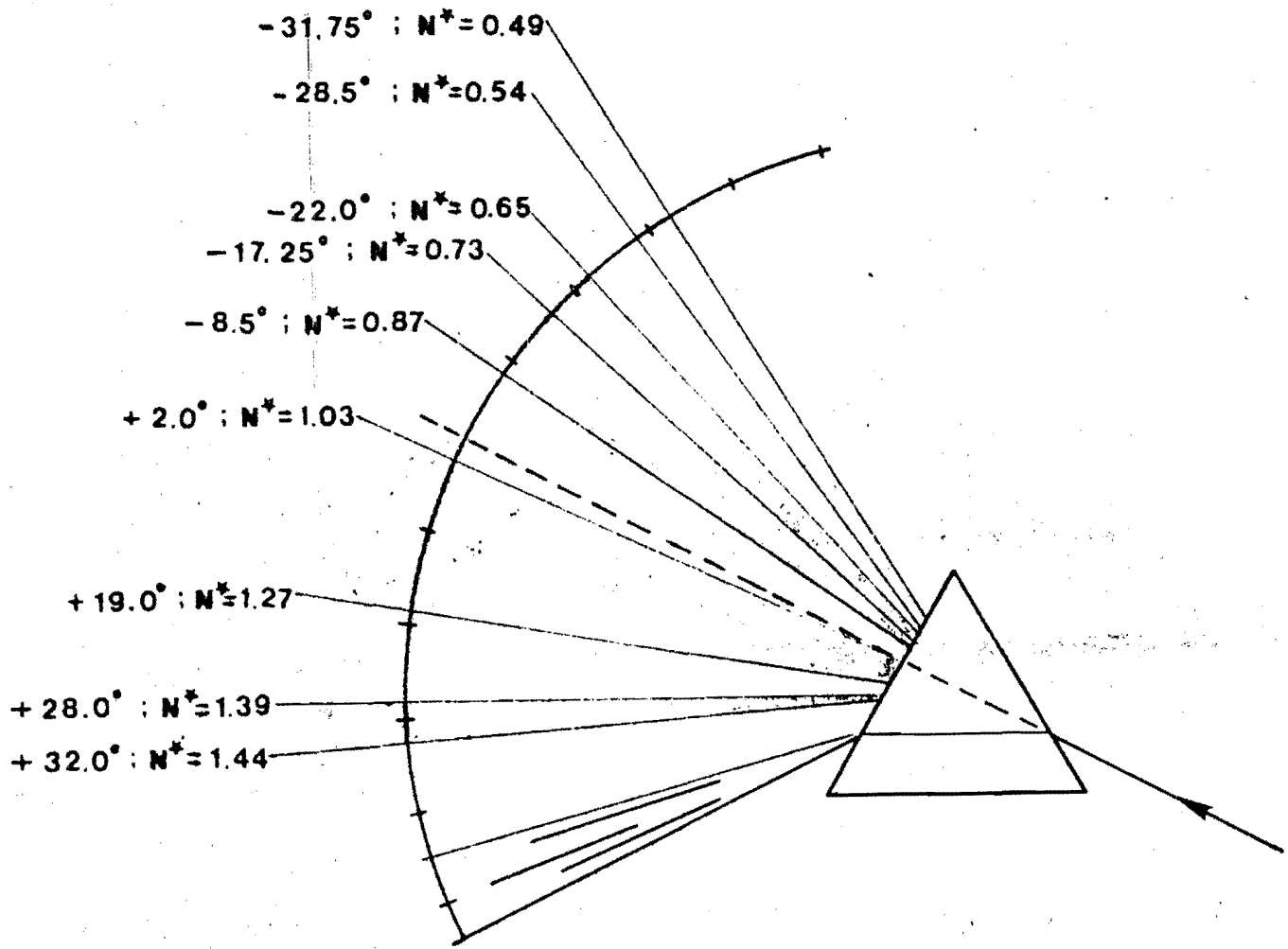

Fig. 13. Spectral dispersion of (-) s/t radiation as perceived by Bobby S. (Colors reading clockwise are red - yellow - green - dark green - blue - red - yellow - green).

Also, reviewing the data for which $A = 45^{o}$, one obtains

$$1.42 \geq N_1^* \geq 0.28 \quad .$$

Tabulation of the inequalities in terms of predicted and observed ranges gives

	Prism : $A = 60^{o}$	Prism : $A = 45^{o}$
Predicted range - - - -	$1.648 > N_1^* \geq 0.16$	$1.577 > N_2^* \geq 0.36$
Observed range - - - -	$1.55 \geq N_1^* \geq 0.48$	$1.42 \geq N_2^* \geq 0.28$.

From the tabulation for prism : $A = 60^{o}$, the observed range is contained within the predicted range. For the prism : $A = 45^{o}$, the upper end of the observed range is contained in the expected range. The lower end of the observed range, however, is not contained within the lower end of the predicted range. Closer review of the data of Table 2 shows that, for the latter case, the next value greater than $N_2^* = 0.28$ is $N_2^* = 0.45$, which is within the predicted range. In making the previous comparison, one must keep in mind that the measured N values were obtained by use of the bright yellow line of the sodium light source. From the N values, the conjugate N^* values were computed. Since the light source used in the N^* experiments was an incandescent one, the associated frequency differences must be considered in making the comparisons.

It is of interest to note, from the observed data, that $N > N^*$ is as predicted. This prediction actually came about from the data of the telescope phenomena[2]. Though there were slight magnifications of the observed

auric images in the telescope work, the magnification values were always less than the physical magnification of the telescope. In fact, it was concluded that such a result could not occur since to do so would require the subject to see physically and aurically simultaneously. This is apparently impossible because seeing aurically is a consequence of appropriately altered physical eyesight. This reasoning led to the conclusion that the same thing would happen in the case of the N^* work; i.e., $N > N^*$.

From a review of Figs. 9-13, some important observations can be drawn from the spectral aspects of this phenomena. In Fig. 8, theory predicts that the conjugate spectrum (colors indicated by * superscripts) will be inverted from that of the physical spectrum. In Figs. 9, 10 and 13, the spectral order is the same as predicted in Fig. 8. Figures 11 and 12, however, show that at least part of the spectral order is reversed. There is no known explanation for the reversed order. A clue might be obtained by noting the multiple spectra (octaves) results obtained in Fig. 13. Thus, it could possibly be that the subjects were actually seeing the partial spectra from a given octave overlapping the partial spectra of another higher order octave. Such a result would lead to the impression of a reversed spectral order as seen in Figs. 11 and 12.

The results presented in Fig. 13 seem to be a unique case and consequently deserve more detailed discussion. First, it is noteworthy that this particular subject, Bobby, was the most sensitive of the subjects to this type of phenomena. Perhaps the results, as presented in the figure, express this fact. In addition to the data in this figure, there was one bit of information

not included for clarity reasons. After Bobby started and ended his observations at $+32.0^{o}$ and -31.75^{o}, respectively, he subsequently returned to an arc region that had previously caught his attention. This region was the angular arc from -23.0^{o} to -28.25^{o}. In this small arc of 5.25^{o}, he reported seeing another octave containing the colors as previously seen. Thus, three distinct spectra or octaves occurred. These results suggested some interpretive analysis based upon a diffraction grating.

The diffraction grating is an optical device widely used in place of a prism to study the spectrum. The essential difference between this spectrum and the one from a prism is that the diffraction grating produces several images of the same spectrum; whereas, a prism confines all the light to one. The different images are produced by wave fronts emerging from the grating and interfering with other fronts propagating in a different plane. The resulting images or spectra are referred to as the 0, 1st, 2nd, etc., orders of interference. Because the width of each spectrum is proportional to its order, the higher order spectra become wider and overlap each other more and more. These considerations provide some interesting analogies relative to the spectral results presented in Fig. 13. First, one notes that instead of just one spectrum being produced with the prism, three were actually perceived by this subject for the (-) s/t radiation. This suggests that a diffraction grating mechanism is operating. If we assume this to be the case, another unusual feature is noted to exist. Let us assume that the 0 order to central image is that of the physical refracted light in our experiment. Then, according to Fig. 13, and opposite to the physical diffraction grating, the three orders were narrower the higher the order. This implies that the

(-) s/t mirror principle is operating. Thus, in Bobby's case, the phenomena appear to act like conjugate aspects from a diffraction grating.

From the (-) s/t theory, it is quite clear that mirror image results are predicted. This expectation, however, appears to contrast with some of the results from the telescope phenomena and the N^* values. These data suggest that there are apparently many mental or consciousness states being expressed. On the basis of human experience, this is not unexpected. That is, in the mental transition from the fully conscious state ((+) s/t) to an extreme altered state ((-) s/t), many intermediate states are encountered. All evidence indicates that both extremes do not exist simultaneously and that the suppression of the one leads, as a consequence, to the amplification of the other. They do appear to be intimately connected and the foregoing considerations might resolve the contrast.

These considerations lead to a conceptualizing model that attempts to express this relationship (see Fig. 14). Though we cannot be sure of the true interrelationship between these two systems, the one of Fig. 14 suffices for the present. The graph of $y = f((+)s/t)$ represents a model of the behavior of the (+) s/t sensory system and $y^* = f((-)\ s/t)$ that of the (-) s/t sensory system. The graph base represents relative consciousness states and the two vertical axes depict the relative degree within that state. Since the two systems are conjugates of each other, they will have mirror image symmetry. This feature is obtained in Fig. 14 by folding the page from left to right at state 2. That is, y maps onto y^*. At the arbitrary consciousness state 1, y is a relative maximum and y^* is a relative minimum.

Similarly, at state 4, y^* is a relative maximum while y is now a relative minimum.

From the foregoing description, there are many intermediate states between points 1 and 4 (Fig. 14). Subjects under test could be mentally operating at any one of many possible states within the indicated boundary. However, from the standpoint of human experience, we would expect that states toward the right, along the graph base, to be more conducive to producing the so called "psychic event." Similarly, those states more to the left would be the "fully conscious" or "nonpsychic" state.

Carlton has suggested that the network of the physical human sensory system may be one-and-the-same as that used by the (-) s/t sensory system[3]. In the (+) s/t sensory system, information flows from an external origin to the eyes, ears, nose, etc., and internally to the brain. For the conjugate sensory system, the energy flows in the opposite direction. Thus, if both sensory systems tried to operate simultaneously to a high degree while using the same physical sensory network, there conceivably would be a destructive interference and subsequently one of the two could win out. The model of Fig. 14 allows for this to happen.

Without doubt, this model has many weaknesses. Even so, it may have some practical utility. For example, if total loss of consciousness accompanies or perhaps precedes physical death, one may ask--What does the model have to say about this case? Certainly there can be no consciousness at death. From the model, this condition is reached when $y = 0$. At this condition, has y^* continued in an unbounded fashion? We do not know for sure but there are

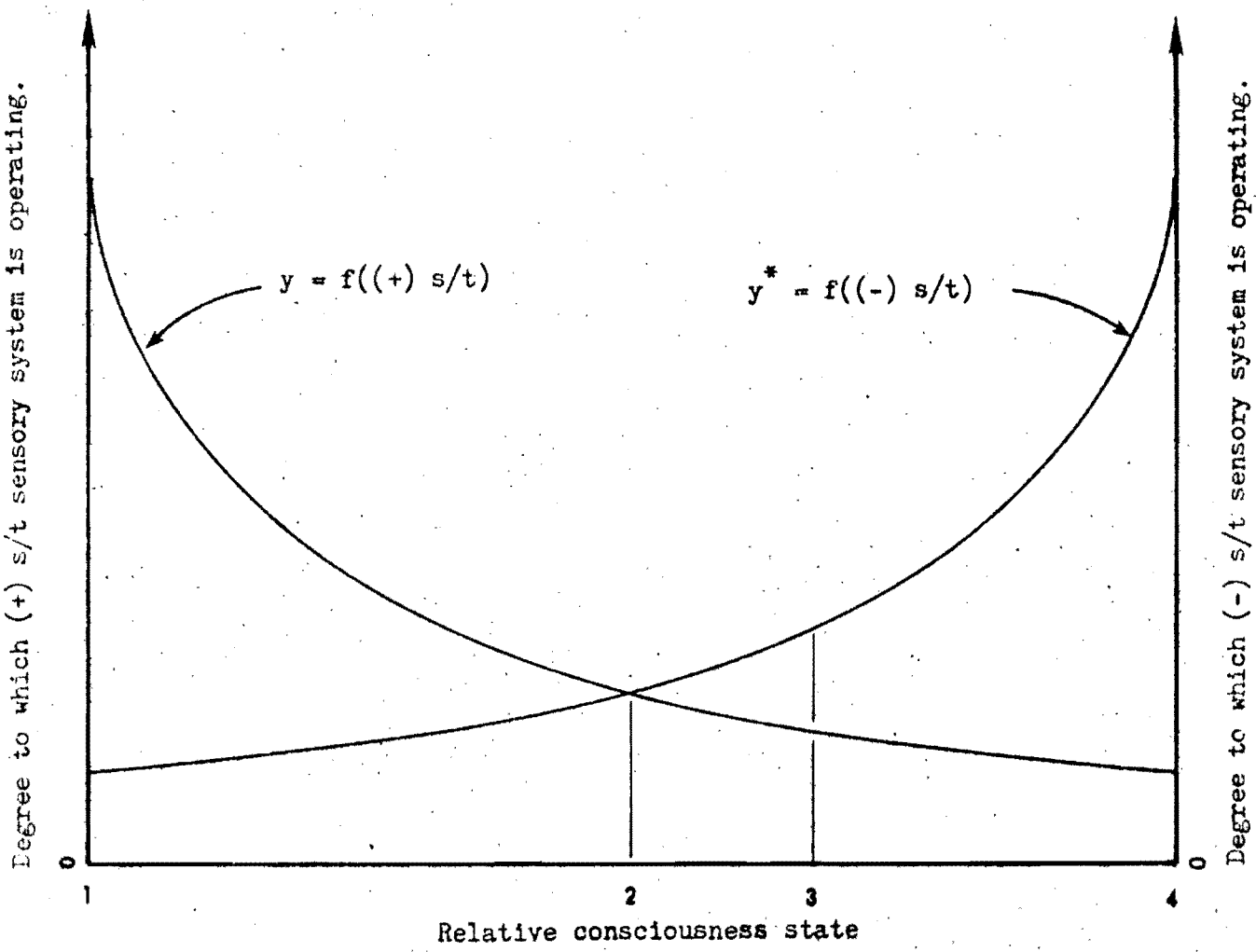

Fig. 14. Graph of a conceptualizing model to illustrate the general interfacing nature of the (+) vs (-) s/t human sensory systems.

some insights about this from the (-) s/t theory. The human psyche appears to have the ability to construct holograms in the (-) s/t frame; i.e., this is what the subjects have been doing in the index-of-refraction studies. Since every physical object has a conjugate that exists in the (-) s/t frame, then so does the human body have such a conjugate or hologram. From the (-) s/t theory, holograms are constructed and exist prior to the physical manifestation of them. Consequently, the (-) s/t hologram is fundamental to everything physical. Thus, if the hologram exists before and independent of its physical manifestation, then it should exist after its physical manifestation. For example, the hologram for the law of gravitation continues to exist even after it has physically manifested itself infinitely throughout history. These considerations lead us to suspect that as y approaches 0, y^* approaches a maximum and, as such, the individual human identity (spirit) is completely absorbed or contained in its (-) s/t hologram--a natural condition or transformation that takes place in the direction of a more fundamental essence.

References

1. Carlton, J. B., Experimental Techniques in Human Aura Analysis (Proceedings of the Seventh Annual Medical Symposium on New Horizons in Healing, Jan. 23-27, 1974, A.R.E. Clinic, Inc., Phoenix, Arizona).
2. Carlton, J. B., The Telescope Phenomena: Running Around at Velocities Violating the Speed Limit of Light (Proceedings of the Eighth Annual Medical Symposium on The Healing Mechanism: An Adventure in Consciousness, Jan. 22-26, A.R.E. Clinic, Inc., Phoenix, Arizona).
3. Carlton, J. B., Insights into the Role of Body Energies Through Auric Phenomena (Proceedings of the Ninth Annual Medical Symposium on Holistic Patient Care and the Role of Body Energies, Jan. 21-25, 1976, A.R.E. Clinic, Inc., Phoenix, Arizona).
4. Tiller, W. A., The Positive and Negative Space-Time Frames as Conjugate Systems (Proceedings of the Eighth Annual Medical Symposium on The Healing Mechanism: An Adventure in Consciousness, Jan. 22-26, 1975, A.R.E. Clinic, Inc., Phoenix, Arizona).
5. White, H. E., Modern College Physics (D. Van Nostrand Co., Inc., New York, Second Editiion, 1953).
6. Tiller, W. A., A Lattice Model of Space and Its Relationship to Multidimensional Physics (Proceedings of the Tenth Annual Medical Sympsoium, January 1977, A.R.E. Clinic, Inc., Phoenix, Arizona).